Section A-Research paper

A Comparative study on structural, morphological and optical properties of ZnO thin films deposited by Jet Nebulizer Spray Pyrolysis and Sonicated Nebulizer Assisted Atomizer Pyrolysis

P.S. Vinod [a], V. Ponnuswamy [a,*], C. Sankar [a], S. Vivekanandhan [b].

[a] Department of Physics, Sri Ramakrishna Mission Vidyalaya College of Arts and Science, Coimbatore-641 020, India.
[b] Department of Physics, V.H.N.S.N. College, Virudhunagar- 626001, India.
[*]Corresponding author. Tel.: +91 4222692461; Fax: +91 4222693812;
E-mail address: ponnsv007@gmail.com (Dr. V. Ponnuswamy).

Abstract

The films prepared through JNSP (Jet Nebulizer Spray Pyrolysis) and SNAAP (Sonicator Nebulizer Assisted Atomizer Pyrolysis) are studied. The physical properties of the samples are studied to line out the efficious method. SNAAP ZnO films has high intensity XRD peaks with better crystallinity, high transmittance, low absorption, values of texture coefficients greater than unity and nonobotic structures like butterfly. The size of the Crystal, dislocation density, microstrain and band gap are also examined. Among the samples of the study the films prepared by SNAAP method exhibits better physical properties such as transmittance (98%), band gap (3.0 eV), crystal size (9.28 nm) and micro strain (1.8 x 10^{-3} (line^{-2} cm^{-4})). The voidless nano structures and improved physical attributes of the thin films are highly useful for the development of devices like diodes and solar cell.

Introduction

Material science is an interdisciplinary domain of research which investigates the properties of materials and its design [1]. Nanotechnology is a type of engineering that deals with the properties and applications of a nanosized materials [2]. Nanotech has numerous comprehensive application oriented researches with high potential and commercial benefits. These distinct features of nanotech captivates the interest of researchers and academicians. The prime hotspot of nanotechnology is thin film technology, which constitutes a layer of materials ranging from fractions of nanometer to several micrometer in thickness [3]. The extensive assortment of application established on thin films are diodes, transistors, gas sensors, photovoltaic devices, solar cells, architectural coatings, anti-reflective coating in smart phones, laptops etc. Thin films are built upon the process of deposition. Various deposition methods and techniques like pulsed layer deposition [4], electrochemical deposition [5], sol-gel technique [6], laser ablation [7], electron beam evaporation [8], vacuum thermal evaporation [9], ion beam sputtering [10], magnetron sputtering [11], spray

pyrolysis [12], jet nebulizer spray pyrolysis [13] are employed to fabricate thin films. The effectiveness of coating method ameliorates the attributes of thin films. The current paper focus on the sonicated nebulizer assisted atomizer pyrolysis deposition for its high productive nature. It is a cost effective and simple deposition method which aids in large scale production. The present study compares the thin films prepared by sonicated nebulizer assisted atomizer pyrolysis (i.e., sonicated sample) and jet nebulizer spray pyrolysis (i.e., nonsonicated sample). To line out the most effective method of deposition their structural, morphological and optical properties are examined.

Experimental procedure

The samples of the study are prepared by the following procedure. To coat the thin film, a precursor solution is prepared. Which constitutes 0.2195 g of zinc acetate and 10 ml of diluted ethanol. The alcoholic solvent, ethanol is diluted in 1:1 ratio. The prepared precursor solution is constantly stirred using a magnetic pelletizer coupled with ultrasonic stirrer unit. In order to obtain a transparent solution, while stirring milky white precursor solution the acetic acid is gradually added for about twenty minutes. The preheated glass substrate is coated with a prepared solution using a nebulizer spray gun along with the ultrasonic probe. The other sample is fabricated using JNSP method.

Structural properties

The X-ray diffraction patterns of sonicated and nonsonicated ZnO thin films are shown in figure 1. The diffraction peaks of both the prepared samples are based on the scanning angle (2θ) 31.75°, 34.45°, 36.25°, 47.55°, 56.65°, 62.85°, 66.38°, 67.96°, 69.10°, 72.56° and 76.95° which are in congruence with the *hkl* plane value (100), (002), (101), (102), (110), (103), (200), (112), (201), (004) & (202) respectively. This reveals the polycrystalline nature of ZnO thin films. The diffraction peaks of both the samples are in accordance with JCPDS card 36-1451. In which, the sonicated

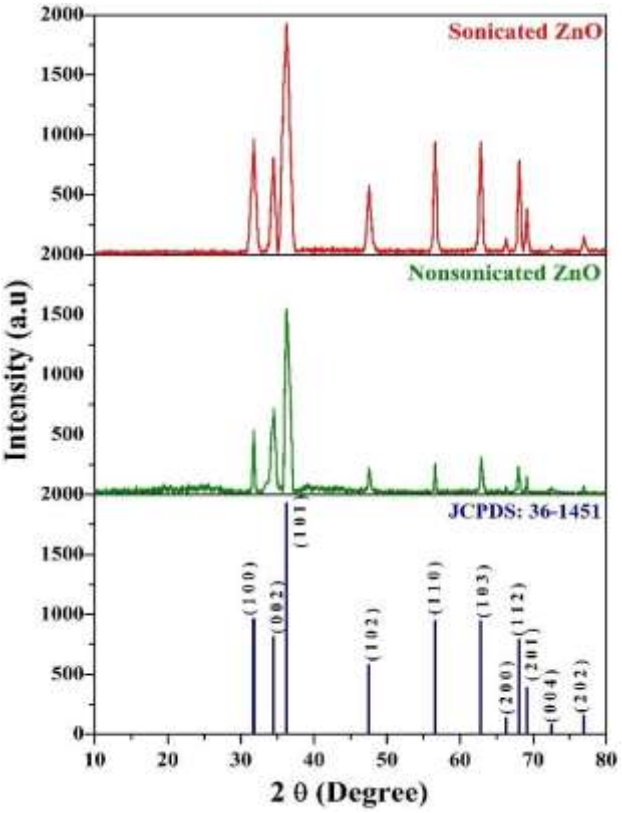

Fig. 1 XRD patterns Sonicated and Nonsonicated thin films.

sample has more elevated peak intensities when compared to that of nonsonicated sample. This apparently indicates that the improved preferential c axis growth of the prepared films that are in perpendicular to the substrate's surface. No other diffraction peak other than ZnO can be found this is due to the alcoholisation of zinc acetate in the precursor solution which indeed confirms the hexagonal wrutize structure. The *hkl* plane (101) seems to be the common highest peak of both the sonicated and nonsonicated sample. The aggravation of growth intensity in (101) plane is closely associated with the process of sonication. In opposition to that of a nonsonicated sample, the preferential orientation of the sonicated thin films are aggravated with the varied increasing intensities. The weak diffraction peaks such as (200) (004) (202) of thin films in a nonsonicated samples are enhanced when the process of sonication is applied to it. As a result of which the crystallite size decreases along with the increase in strain and this serves to be the reason for better crystalinity in the sonicated films.

Crystallanity

The Crystalanity of the samples are analysed using the Debye- Scherrer's equation [14, 15].

$$D = \frac{0.9}{\beta \cos \theta}$$

In which λ represents the wavelength of X-ray (1.5406 Å), β represents the full width at half maximum, theta represents the bragg's angle, and D represents the size of the grains. The crystalanity of the sonicated sample is effectively high when compared to that of a nonsonicated sample, which is represented in figure 2. For nonsonicated sample the grain size of the prominent peak (101) is 18.57 nm whereas for the sonicated sample, the grain size is 9.28 nm. The average grain size of sonicated sample (21.23 nm) is comparatively

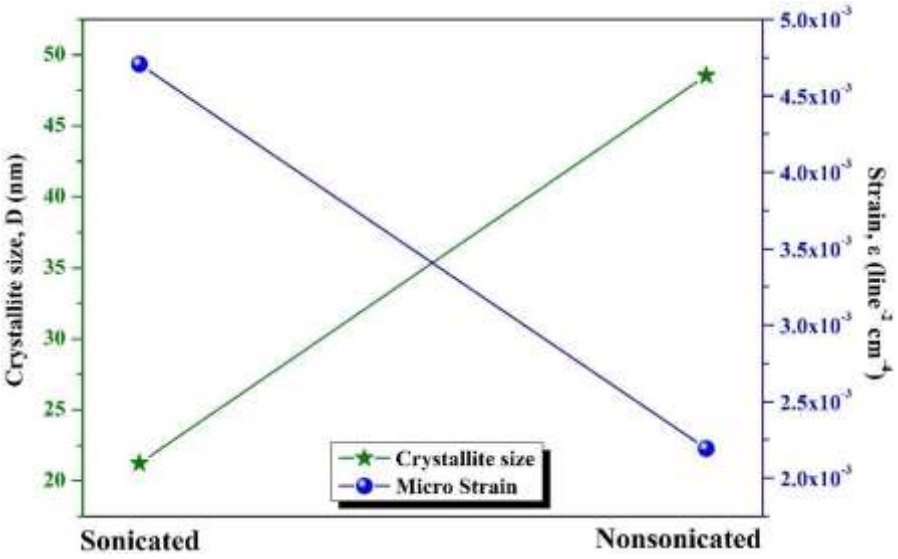

Fig 2. The plot of Crystallite size and Strain.

low when compared against the average grain size of a nonsonicated sample (48.52 nm). This is due to the process of sonication. In which ultrasonic wave agitates the particle of the precursor solution and that helps in fine coating of the films.

The dislocation density (ð) of the samples are calculated using Williamson and Smallman formula[16]

$$\delta = \frac{15\,\varepsilon}{aD} \text{ lines / m}^2$$

The average dislocation density (δ) of the sonicated and nonsonicated films are 3.31 x 10^{-3} (10^{10} lines/m^2) and 7.62 x 10^{-3} (10^{10} lines/m^2) respectively.

The microstrain (ε) of the samples are computed using the relation[17],

$$\varepsilon = \frac{\beta\,\mathrm{Cos}\theta}{4}$$

The microstrain of a nonsonicated sample is 8.55 x 10^{-3} (line^{-2} cm^{-4}) and the sonicated sample is 1.84 x 10^{-3} (line^{-2} cm^{-4}) as because the strain decreases along with decrease in size of the grain the crystallinity of the Sonicated sample is found superior.

Texture Coefficient

The orientation of the crystals can be estimated through the equation of Texture coefficient (T_c) [18,19].

$$\mathrm{Tc} = \frac{\mathrm{I_s}(hkl)/\mathrm{Io}(hkl)}{\sum_n \mathrm{I_s}(hkl)/\mathrm{Io}(hkl)}$$

Where Io and Is are the obtained and standard intensity. The figure 3 represents the values of a texture coefficient for both the sonicated and nonsonicated thin films. In which, the peaks of the sonicated sample has its Tc value greater than unity and that signifies the better crystal orientation. It also confirms the growth of a crystal in c-axis direction. Nonsonicated sample has nonlinear Tc values when compared to that of a sonicated samples. In nonsonicated sample only two prominent peaks (002) and

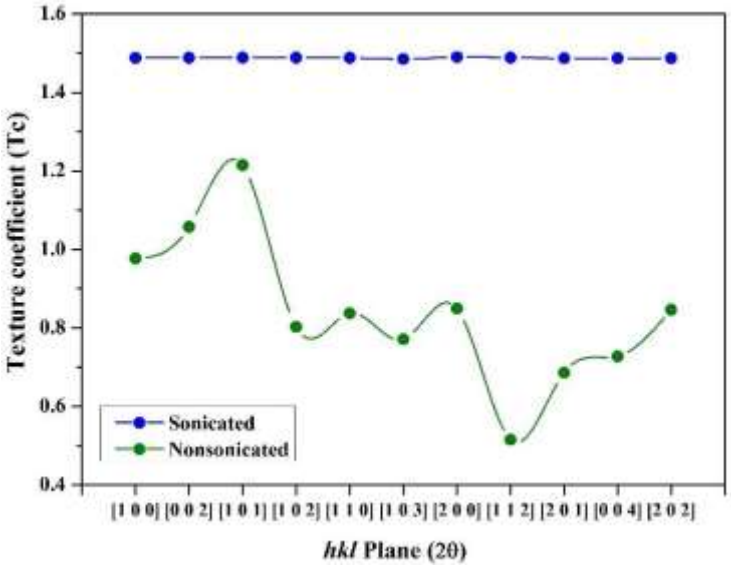

Fig 3. The plot of Texture coefficient and *hkl* plane.

(101) has its Tc value greater than unity but in sonicated sample all the peaks are prominent with high Tc values. Thus, the sonicated sample shows better crystal orientation when compared against the nonsonicated sample.

SEM

The surface morphological analysis (FESEM) of the sonicated and nonsonicated ZnO thin films are shown in figure (4A - 4D). In which, the figure 4A and 4C represents the SEM nanographs of higher magnification; figure 4B and 4D represents the SEM micrographs of lower magnification. The thin films prepared by both the methods are uniformly coated all over the substrates. In figure 4B, the voids and few agglomeration of grains can be significantly noticed. Comparatively in the prepared sonicated sample (figure 4D) at micro level, the grains are invariably deposited and grown in c-axis direction to unveil the presence of nanobutterfly structure within it. To reconfirm the prestine nature of the Sonicated films, the SEM image is further magnified to 100nm (figure 4C), which results in the flawless fluttering nanobutterfly structure without any pores and agglomeration. Though, the deposited grains looks uniform on substrate (figure 4B), the size of the grains differ from 22.17 nm to 77.16 nm. Thus, the nano graphs of nonsonicated sample exhibits varied surface morpologies like nano flowers, nano buds and nano leaves in figure 4B. While comparing the sonicated and nonsonicated

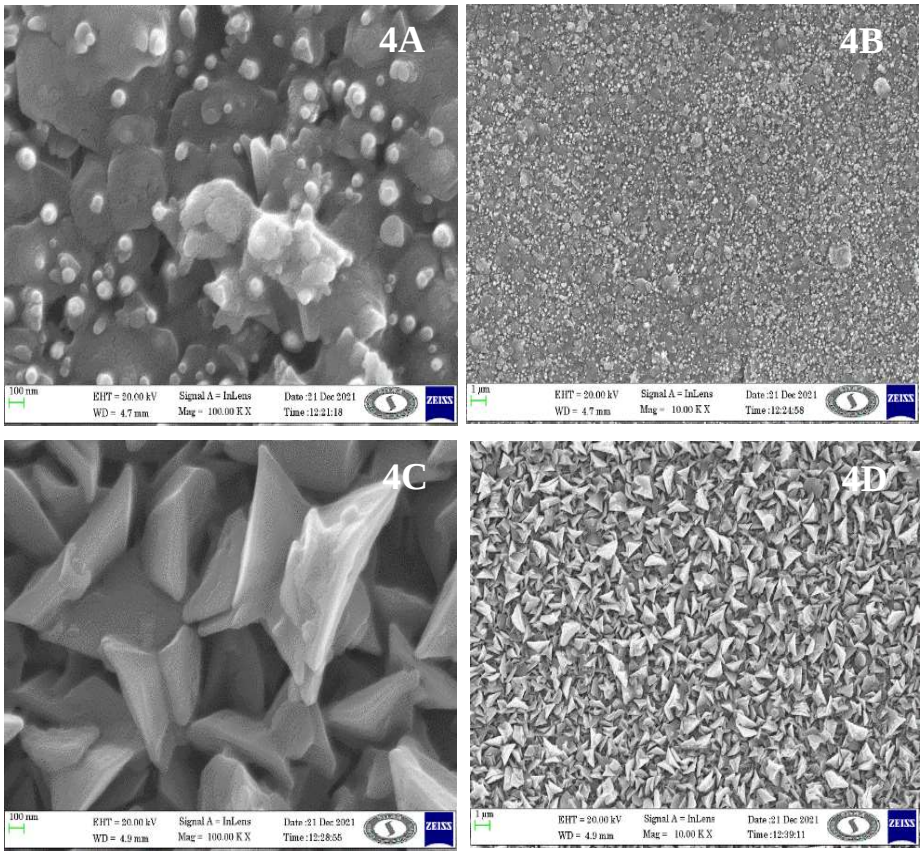

Fig. 4A and 4B. The SEM images of nonsonicated sample.

Fig. 4C and 4D. The SEM images of sonicated sample.

samples, the sonicated sample serves at its best. Sonicated samples has a well-defined nano structures and consistent particle size which does not vary in magnification. The process of sonication aids in the consistent retention of grain size, reduction of voids, clustered grains and cracks.

Transmittance

The spectral transmittance of the sonicated and nonsonicated thin films with the wavelength from 300 nm to 1800 nm are shown in figure 5. The value of transmittance for sonicated sample is 98% and the transmittance value of nonsonicated sample is 82%. Though the high transparency of both the sample lies in visible region. The value of transmittance for sonicated sample is high when compared against the nonsonicated sample. High transmittance of sonicated sample results in higher crystalinity and low absorption. The average value of transmittance are 95.25% and 83.30% for sonicated and nonsonicated sample respectively. The highest average transmittance is obtained for the sonicated sample. Thus, the process of sonication improves transmittance.

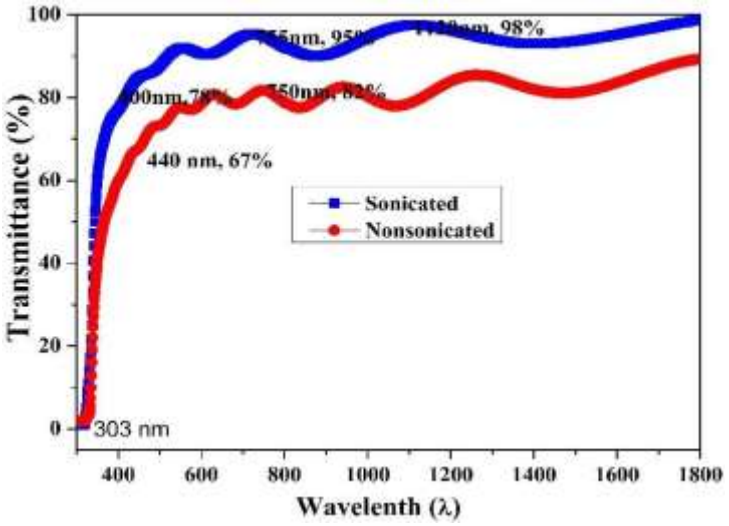

Fig 5. The transmittance vs wavelength plot.

Bandgap

In figure 6 the Tauc's $(\alpha h\nu)^2$ vs. $h\nu$ plot [20] is drawn in order to calculate the Bandgap (Eg)

$$\alpha h\nu = A\,(h\nu - E_g)^{1/2}$$

Where $h\nu$ is photon energy, A is the constant and α is the absorption coefficient. The optical bandgap value of sonicated and nonsonicated films are 3.0 eV and 3.5 eV respectively. The bandgap value of the nonsonicated

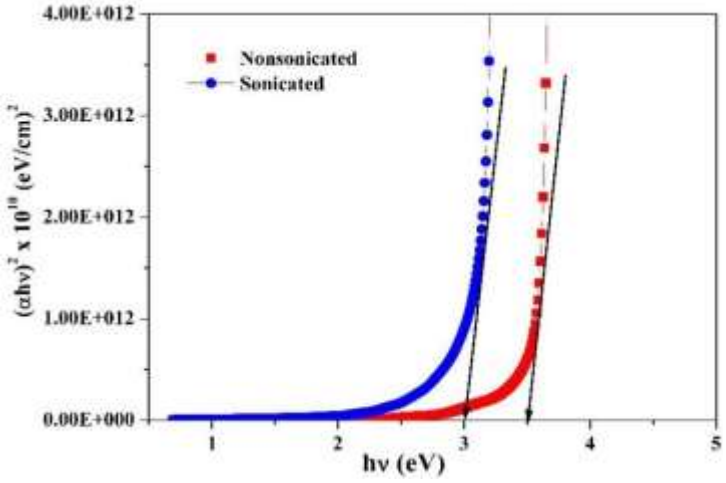

films are reduced when compared with the value of sonicated sample. To obtained bandgap value of the sonicated sample is exactly similar to that of the standard values of ZnO.

Conclusion

The sonicated and nonsonicated samples of ZnO thinfilms are compared. The sonicated Samples has more aggravated peak intensity, better crystallinity, decreased grain size (9.28 nm), microstrain (1.8 x 10^{-3} ($line^{-2}$ cm^{-4})), low absorption, exact bandgap and diminished dislocation density (3.31(10^{10} $lines/m^2$)). The transmittance of the sonicated sample is high (98%) when compared to the nonsonicated sample (82%). The value of texture coefficient is greater than unity with improved crystal orientation. The FESEM images of the sonicated sample reveals the structures of nanobutterflies without any voids and agglomeration of grains. The comparative study results that, the sonicated samples of ZnO thinfilms implicates the preferential attributes for the development of device application.

References

[1] Anter El-Azab, 2017. Why materials theory? Materials Theory, 1(1). https://doi.org/10.1186/s41313-017-0001-5

[2] What is nanotechnology? , National nanotechnology initiative. https://www.nano.gov/nanotech-101/what/definition, (accessed 26 May 2023)

[3] Thin film, Wikipedia. https://en.wikipedia.org/wiki/Thin_film, (accessed 15 July 2023)

[4] Quanhe Bao, Chuanzhong Chen, Diangang Wang, Qianmao Ji, Tingquan Lei, Pulsed laser deposition and its current research status in preparing hydroxyapatite thin films, Appl. Surf. Sci. 252 (2005) 1538–1544. https://doi.org/10.1016/j.apsusc.2005.02.127

[5] Jin-Liang Zhuang, Yan-Min Shen, Yun Xue, Mi Yan, Hu Cheng, Zhuo Chen, Xiu-Jun Yu, Xiao-Bing Lian, Shao-Bin Zhu, Electrochemical deposition of Perylene-Based thin films from aqueous solution and studies of Visible-Light-Driven oxidation of alcohols, ACS Appl. Energy Mater. 3 (2020) 9098–9106. https://doi.org/10.1021/acsaem.0c01475

[6] Sanjeev K. Sharma, Satendra Pal Singh, Deuk Young Kim, Fabrication of the heterojunction diode from Y-doped ZnO thin films on p-Si substrates by sol-gel method. Solid State Commun. 270 (2018) 124–129. https://doi.org/10.1016/j.ssc.2017.12.010

[7] M. Boutinguiza, R. Comesaña, F. Lusquiños, A. Riveiro, J. del Val, J. Pou, Production of silver nanoparticles by laser ablation in open air. Appl. Surf. Sci. 336 (2015) 108–111. https://doi.org/10.1016/j.apsusc.2014.09.193

[8] D. Bromley, A. J. Wright, L. A. H. Jones, J. E. N. Swallow, T. Beesley, R. Batty, R. S. Weatherup, V. R. Dhanak , L. O'Brien, 2022. Electron beam evaporation of superconductor-ferromagnet heterostructures. Scientific Reports. 12, 7786. https://doi.org/10.1038/s41598-022-11828-y

[9] A. U. Moreh, M. Momoh, H. N. Yahya, B. Hamza, I. G. Saidu, S. Abdullahi , Effect of thickness on structural and electrical properties of CuAlS2 thin films grown by two stage vacuum thermal evaporation technique, Int. J. Math. Sci. 8 (2014) 1084–1088. https://doi.org/10.5281/zenodo.1338963

[10] B. Ziberi, M. Cornejo, F. Frost, B. Rauschenbach, 2009. Highly ordered nanopatterns on Ge and Si surfaces by ion beam sputtering. J. Phys.: Condens. Matter. 21, 224003. https://doi.org/10.1088/0953-8984/21/22/224003

[11] Yuan Tian, Lianguo Gong, Xueqian Qi, Yibiao Yang, Xiaodan Zhao, Effect of substrate temperature on the optical and electrical properties of Nitrogen-Doped NiO thin films, Coatings. 9 (2019) 634. https://doi.org/10.3390/coatings9100634

[12] Vinay Kumar Singh, Thin film deposition by spray pyrolysis techniques, J. emerg. technol. innov. res. 4 (2017) 910–918.

[13] S. Marikkannu, M. Kashif, A. Ayeshamariam, N.Sethupathi, V. S. Vidhya , S. Piraman , M. Jayachandran, Studies on jet nebuliser pyrolysed indium oxide thin films, J. Ovonic Res. 10 (2014) 115–125.

[14] Ensnaring animate-inanimate toxins using ZnO–MgO @ Elastomer thin films with self-cleaning and regenerative properties, Environ. Technol. Innov. 24 (2021) 102011. 10.1016/j.eti.2021.102011

[15] Optimization of physical properties of sputtered silver films by change of deposition power for low emissivity applications. J. Alloys Compd. 853 (2021) 57073. 10.1016/j.jallcom.2020.157073

[16] R. Mariappan, V.Ponnuswamy, S.M.Mohan, P.Suresh, R.Suresh. The effect of potential on electorodeposited Cd Se thin films, Mater. Sci. Semicond. 15 (2012) 174–180.

[17] Effect of deposition temperature on the properties of Cu2ZnSnS4 (CZTS) thin films. 103 (2017) 335-342. 10.1016/j.spmi.2017.02.003

[18] Kovalakannan Sivalingam, Prabakaran Shankar, Ganesh Kumar Mani, John Bosco, Balaguru Rayappan, Solvent volume driven ZnO nanopetals thin films: Spray pyrolysis, Mater. Lett. 134 (2014) 47-50.

[19] R. Swapnaa, M. Ashoka, G. Muralidharanb, M.C. Santhosh Kumara, Microstructural, electrical and optical properties of ZnO:Mo thin films, with various thickness by spray pyrolysis, J. Anal. Appl. Pyrolysis. 102 (2013) 68-75.

[20] H. Belkhalfa, H. Ayed, A. Hafdallah, M.S. Aida, R. Tala Ighil, Characterization and studying of ZnO thin films deposited by spray pyrolysis: Effect of annealing temperature, Optik (Stuttg.). 127 (2016) 2336–2340.